INVESTIGAȚII PRELIMINARE ALE UNUI LIANT DE TIP GEOPOLIMER PE BAZA DE DEȘEURI
PRELIMINARY INVESTIGATION OF GEOPOLYMER BINDER FROM WASTE MATERIALS

RUBEN P. BORG[1]*, CHARLO BRIGUGLIO[1], VYTAUTAS BOCULLO[2], DANUTĖ VAIČIUKYNIENĖ[2]

[1] *Department of Construction & Property Management, Faculty for the Built Environment, Built Environment Building, Room 213, University of Malta, Msida, MSD 2080, Malta*
[2] *Kaunas University of Technology, Faculty of Civil Engineering and Architecture, Studentu g. 48, LT-51367 Kaunas, Lithuania*

Concrete produced from ordinary Portland cement (OPC), is a building material with wide applications, due to various factors, including strength and durability characteristics. Nevertheless, OPC concrete has a significant environmental impact due to resource consumption and energy intensive production of the cement as a result also of the high temperatures during manufacture. The main factors that affect the geopolymerisation process include the type and characteristics of the raw materials, the alkaline activators and the curing conditions. The optimum alkaline solution used and activator, to raw material mass ratio depend on the type and characteristics of the raw materials being used. Furthermore, the curing conditions adopted depends on the characteristics of the raw materials and activators. Industrial by-products and waste rich in SiO_2 and Al_2O_3 can be utilized as raw material for geopolymer concrete. In this research, three different waste materials were considered: Polish coal burning fly ash (FA), Lithuanian biomass bottom ash (BMBA), AlF_3 production waste (PW). Paste was produced to determine the influence of the Al_2O_3/Na_2O ratio on the geopolymer paste properties. The material properties were determined for the curing conditions set with respect to X-Ray diffraction characterisation (XRD), Helium Pycnometry (HP) and Mercury Intrusion Porosimetry (MIP) and compressive strength.

This research shows that, the three waste materials analysed, all have great potential for use as a geopolymer concrete, to varying degrees. It was further determined that the mix ratios and the curing environment are critical for the performance of the material in cast in situ and precast concrete applications.

1. Introduction

The production of Ordinary Portland cement is a primary source of CO_2 emissions within the construction industry. Ordinary Portland cement is used as a primary binder in concrete elements. Cement production and use are on the rise with increasing needs of different types of concrete in buildings and infrastructure. Part replacing of cement with an alternative material, which is based on production waste, can improve the impact on the environment in two ways: reduction in cement production, therefore, less CO_2 emissions and reduction in waste material disposed of in the environment, as this will be used as a binder instead of Ordinary Portland cement. What is today perceived as production waste will be further utilized by prolonging the life cycle of a waste material and converting such waste into a resource.

2. Geopolymer Concrete

Several studies have been carried out in the past decades on the potential replacement of Portland cement with an alternative, more sustainable material with a lower impact on the environment, [1]. Research on the use of geopolymer as an alternative material to Ordinary Portland cement has increased in the last decades mainly focusing on mechanical properties and characteristics of geopolymer concrete [2]. A geopolymer material has been referred to as an amorphous inorganic polymer that forms the ionic bonding reaction between an aluminosilicate material (Al-Si) and an alkaline solution.

The geopolymer forms with the use of raw material, a SiO_2 and Al_2O_3 source, in the presence of the alkali activator solution. The SiO_2 and Al_2O_3 start leaching into solution leading to poly-condensation and Si^{+4}, Al^{+3} ions, start forming a three-dimensional network of geopolymer chains. The three-dimensional network is the newly formed solid that binds the material together [3]. The activation of silicates increases the dissolution of raw materials resulting in improved mechanical properties.

The mixing proportions are key in geopolymer materials and different operations are presented in

---

* Autor corespondent/*Corresponding author*,
E-mail: ruben.p.borg@um.edu.mt

research as a result of the chemical structure of the precursor material used. Various approaches are presented in literature with regard the mixing proportions, ratios and curing environment for geopolymers. Heath et al. presented the optimum ratios, with respect to the mechanical properties for the particular material, as SiO_2:Al_2O_3 ratios of 3.5 to 4:1 [4]. Rattanasak et al. [5] used ignite fly ash, as a precursor for geopolymer and proposed molar mass ratios as follows: Na_2O/SiO_2 = 0.2−0.48, SiO_2/Al_2O_3 = 3.3−4.5, H_2O/Na_2O = 10−25, Na_2O/Al_2O_3 = 0.8−1.2. The findings of Yusuf et al. [6] revealed that increase in H_2O/Na_2O molar ratios negatively affects the strength but improves the mixture workability. The microstructural morphology examination reveals the contribution of H_2O/Na_2O molar ratios to the product nature, compactness, and the reactivity of Ca^{2+} and Al^{3+} while H_2O/Na_2O ratios contributed to the product amorphousity and carbonation process.

The most common and mostly used activators for geopolymer synthesis are any alkali metals that contain sodium, potassium or calcium (Na, K and Ca). The most common activators used are sodium hydroxide, sodium silicate (water glass) and potassium hydroxide [5]. Van Jaarsveld et al. [7] concluded that the alkali metal cation controls and affects almost all stages of geopolymerization, from the ordering of ions and soluble species during the dissolution process to playing a structure-directing role during gel hardening and eventual crystal formation.

The curing of geopolymer is also a factor that can affect the mechanical properties of the samples. The most common bracket of curing temperature was found to be between 40 °C to 85 °C. Several researchers referred to different curing conditions and temperatures, depending on what the research was focusing on. Mikoč et al. [8]analysed samples in two curing conditions, one set cured at room temperature and the other set steam cured for 8

hours and left at room temperature until testing. The steam cured samples reached compressive strength after 3 days, which was 389% stronger than the samples cured at room temperature. This shows that curing does affect the strength of geopolymer [8]. Pan, et al. 2013 [9] suggest that the best curing condition was in the range of 50 to 80 °C, rather than normal room temperature. It was also suggested that the curing at high temperatures should be an intermediate one for strength development, as long exposure to high temperatures could cause a reduction in strength due to dehydration and excessive shrinkage. Nath ir Rarker [10] aimed to achieve fly ash-based geopolymers suitable for curing without elevated heat. The results show that inclusion of ground granulated blast-furnace slag with type F fly ash helped achieve setting time and compressive strength comparable to those of ordinary Portland cement. Rattanasak et al. [5], analysed the effect of NaOH solution on the synthesis of fly ash geopolymer, with paste and mortar samples cured at 65 °C for 48hrs in plastic containers, and further wrapped in cling film. After the curing period, samples were cured at room temperature until testing.

3. Materials and Methods

In this study, three different waste materials were used: Polish type F coal fly ash, Lithuanian biomass bottom ash and AlF_3 production waste. Chemical composition is showed in Table 1.

Fly ash is one of the coal combustion products, containing fine particles released during combustion with other gases. Fly ash is divided into F type (>5% CaO) and C type (15-35% CaO) according to ASTM standard, depending on the quantity of CaO in the material composition. F type fly ash mainly consists of SiO_2 and Al_2O_3 in aluminate glass form [11].

Table 1

Chemical composition of raw materials. * FA is F type fly ash, ** BMBA is biomass bottom ash and *** PW is AlF_3 production waste

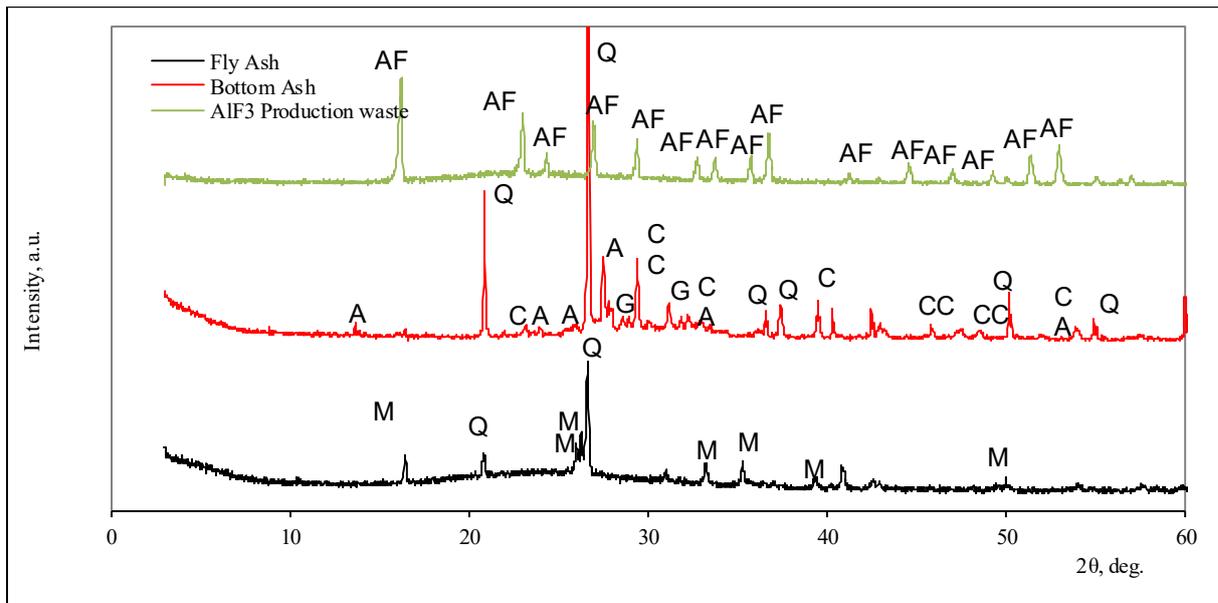| Oxide	weight, %			Oxide	weight, %		
	FA*	BMBA**	PW***		FA*	BMBA**	PW***
CaO	3.683	48.978	0.42	ZrO_2	0.147	0.039	0
SiO_2	49.468	22.39	72.23	SO_3	0.921	0	0
Na_2O	0.945	0.281	0	ZnO	0.05	0.041	0
Al_2O_3	27.452	2.509	5.68	TiO_2	1.658	0.328	0
MnO	0.063	0.347	0	CuO	0.027	0.02	0
MgO	1.699	8.286	0	NiO	0.031	0	0
K_2O	4.539	8.686	0	PbO	0.038	0	0
Fe_2O_3	7.379	2.179	0.66	Cl	0	0.04	0
BaO	0.436	0.161	0	Rb_2O	0	0.024	0
P_2O_5	1.310	5.048	0	SO_3	0	0.582	0
SrO	0.106	0.06	0	F	0	0	21.01

Fig. 1 - XRD analysis of raw materials: Q – quartz (SiO_2), CA – calcium oxide (CaO), CC – calcium carbonate (Ca(CO)$_3$), A – anorthoclase, (Na,K)(Si$_3$Al)O$_8$, G – gehlenite (Ca$_2$ Al(AlSiO$_7$)), AF – aluminium fluoride hydrate (AlF$_3$ · 3.5H$_2$O), M – mullite ((Al(Al$_{1,3}$·Si$_{0,7}$·O$_{4,9}$)(O$_4$))

Fly ash type F is considered to be an excellent material to synthesize geopolymers [12-14]. With reference to XRD analysis, the peaks of quartz and mullite refer to the major minerals of this material. The presence of amorphous SiO_2 is identified as a "halo peak" on the XRD graph within 2θ degree range 18° – 30° (Fig. 1). XRF elemental analyses were used to determine the chemical composition of the raw material and the elemental composition was recalculated to oxides. The results are shown in Table 1. High amounts of amorphous SiO_2 and Al_2O_3 makes fly ash the right raw material as a geopolymer binding material. The bulk density of the F type fly ash that has been used in the research is 1.84 g/cm^3 and was determined with helium pycnometry.

Biomass (timber) bottom ash was used in this experiment. The average particle density, determined with helium pycnometer, was found to be 2.24 g/cm^3. XRF elemental analysis was used to determine the chemical composition of raw material. Elemental composition was re-calculated to oxides and is reported in Table 1. It should be noted that BMBA does not require much NaOH in activator solution, because it consists much alkalis (K_2O and Na_2O). According to the XRD analysis (Fig. 1) these minerals: quartz, calcium oxide, calcium carbonate, anorthoclase (Na,K)(Si$_3$Al)O$_8$ and gehlenite (Ca$_2$Al(AlSiO$_7$)) prevailed in the investigated material.

The third material which was used in this research was AlF$_3$ production waste. The largest part of AlF$_3$ production waste consists of $SiO_2·nH_2O$, where SiO_2 is in the amorphous state [15] . It is known that amorphous SiO_2 could be used as OPC additive, because of its pozzolanic properties [16].

AlF$_3$ production waste is a silicahexaflouride acid neutralisation product. This acid is obtained from the manufacture of phosphoric acid. The silicahexaflouride process reaction is as follows:

$$H_2 \cdot SiF_6 + 2Al(OH)_3$$
$$\rightarrow 2Al_{\ 3} + SiO_2 \cdot nH_2O + H_2O + Q$$
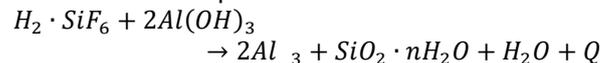
The XRD analysis shows that the material consists of crystalline AlF$_3$ · 3.5 H$_2$O (Fig 2). The XRF analysis shows that the largest part of the AlF$_3$ production waste consist of SiO_2 and Al_2O_3.

4. Research Methodology

The main objective was to assess the potential for replacement of Ordinary Portland cement with waste materials which has a lower carbon footprint. This requires the characterization of the waste material and the determination of its performance characteristics. Transforming a waste material into a resource results in a reduction in waste material generation and a reduction in the consumption of resources. The mix design used for the paste samples is presented in Table 2. In the mixtures design Al_2O_3/Na_2O ratio was changed by adding reagent Al(OH)$_3$. Geopolymers were made with 4 different Al_2O_3/Na_2O ratios: control – without Al(OH)$_3$ reagent and Al_2O_3/Na_2O ratios equal to 0.5, 1.0 and 1.5. Al_2O_3 and alkalis present in the raw materials were also evaluated. In this present research, the curing condition chosen for paste samples were as follows: curing for 24 hours at ambient temperature (20 °C) with the remaining curing period of 28 days in a ventilated oven at a constant temperature of 50 °C.

The compressive strength of the samples was determined using a hydraulic compressive strength machine. For each waste material three samples were cast, in cylindrical mould with a height of 20mm and 20mm in diameter. The compressive strength was determined at 7, 14 & 28 days and for each material with variable addition of Al(OH)$_3$.

Mix design of geopolymer samples. * - control samples without additional reagent Al(OH)₃.

Mixing Ratios			Amounts of raw materials								
			samples with FA			samples with BMBA			samples with AlF₃ PW		
Mix no.	$Al_2O_3/$ Na_2O, molar ratio	$SiO_2/$ Na_2O, molar ratio	Water/ solid mass ratio	FA, wt. %	$Al(OH)_3$, wt. %	NaOH, wt. %	BMBA, wt. %	$Al(OH)_3$, wt. %	NaOH, wt. %	PW, wt. %	$Al(OH)_3$, wt. %	NaOH, wt. %
1	Control*	2	0.25	83	Control*	17	99	Control*	1	77	Control*	23
2	0.5	2	0.25	63	24	13	86	13	1	62	20	18
3	1	2	0.25	50	40	10	73	26	1	49	37	14
4	1.5	2	0.25	41	50	9	64	35	1	40	48	12

Helium pycnometer analyses was carried out on samples prior to the mercury intrusion porosimetry analysis, to obtain the average volume and average absolute density of the sample. The helium pycnometer (HP) characterisation method provides average volume, V_p and average absolute density ρ_{ab} of solids and powder samples. The HP was performed with a Quantachrome Multi Pycnometer, using helium gas as a fluid displacement to determine the volume and density required. Samples were 15 mm height and 6 mm diameter – specially made to fit in the MIP cell.

The mercury intrusion porosimetry (MIP) analysis provides relevant information for the material testing including the porosity, pore size distribution, surface area, particle size distribution, and permeability. The analyses were carried out on each waste material. Tests were performed with a "Quantachrome Poremaster 60", using mercury surface tension of 480mN/m, with an intrusion and extrusion contact angle of 140º.

Mineral composition was analysed using X-ray diffraction. XRD was performed with X-Ray Diffraction, "Bruker D8 Advance", operating at tube voltage of 45 kV and tube current of 40 mA. The source used was copper (Cu). Samples were scanned over a range of 2θ = 5º to 55º, at a scanning speed of 1º/minute.

5. Results and Analysis

The compressive strength of samples was determined for all materials analysed at different aging times. The strength development during the curing period is presented in Figure 2 (a, b, c). The graphs show a scatter but it is clear the additional $Al(OH)_3$ decreases the compressive strength of the samples.

The highest compressive strength was developed in FA samples, while PW samples were the weakest. The BMBA samples with no additional $Al(OH)_3$ after 28 days indicates significantly higher compressive strength then other samples with same
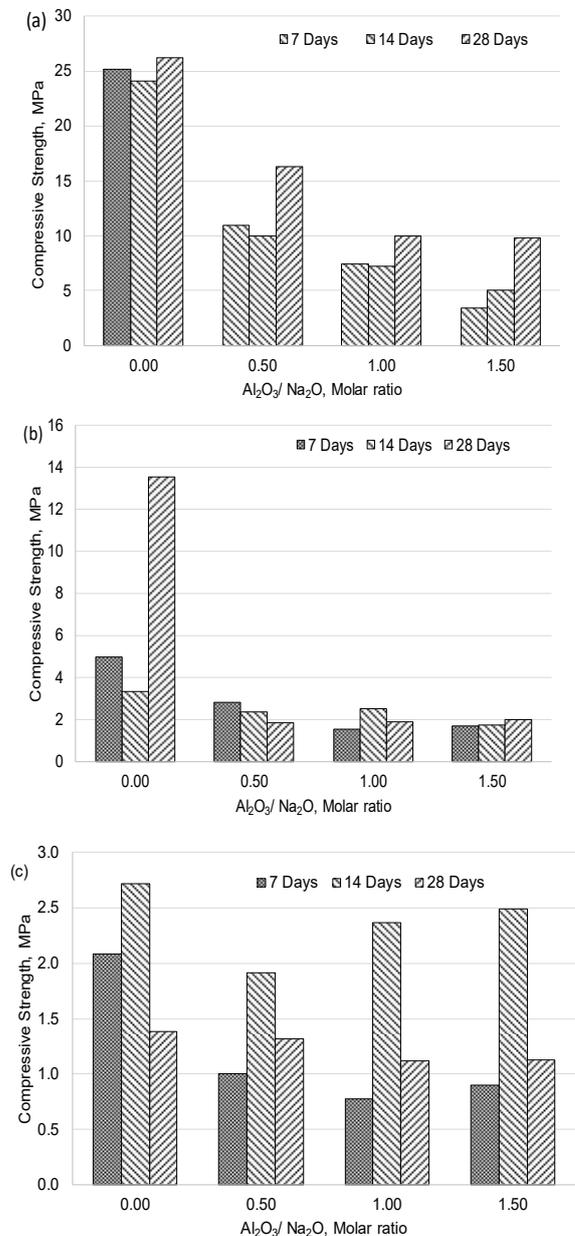

Fig. 2 - Compressive strength of samples by using fly ash type F (a), bottom biomass ash (b) and AlF₃ production waste (c).

materials. In other cases, no drastic increase after the 7 days result was observed. The compressive strength of samples with AlF₃ production waste appears to increase up to 14 days, but with a loss in strength at 28 days. This could be the result of internal cracking of samples because of the long exposure to high temperature. It is noted that the reduction in strength is at 1 MPa – 1,5 MPa, a relatively small difference when compared to bottom ash samples, with a gain in strength of 10 MPa after 28 days.

Additional Al(OH)₃ led to a reduction in strength of the samples as is clearly shown for biomass bottom ash and fly ash samples. Saidi et al. who studied Si/Al and Na/Al ratios influence on properties of geopolymer suggests that stronger Si-O-Si bonds form instead of Si-O-Al when there is less Al content [17].

Samples with AlF₃ production waste were characterised by a low development in strength. It was shown by Pan et al. that long exposure to high temperatures can cause dehydration of the samples and excessive shrinkage, weakening the material [9].

XRD patterns of geopolymers are normally identified through a featureless hump centred approximately at 27° to 29° 2θ (Fig. 3). This hump is mostly known as a diffuse halo peak, which is attributed to the amorphous aluminosilicate gel and which most authors assume to be the primary binder present in geopolymer systems [16]. High intensity peaks determine the crystalline minerals present in the sample. In samples with type F fly ash a common peak was observed in mix 2 (Al₂O₃/Na₂O = 0.5), mix 3 (Al₂O₃/Na₂O = 1.0) and mix 4 (Al₂O₃/Na₂O = 1.5) (Table 2) at 18° 2θ, which shows the greatest intensity for higher Al(OH)₃ quantity levels [19].

The mix 1 (control) showed a diffuse halo peak at around 24° to 36° 2θ, confirming that the

major phase of geopolymer was amorphous. The mix 2 pattern showed a weaker halo peak pattern that tended to slightly disappear in mix 3 and mix 4. This showed that the addition of Al(OH)₃, did not contribute to the geopolymerisation process and this was further confirmed through the compressive strength results, which showed a decline in strength with the addition of Al(OH)₃ in the mix.

Moreover, mix 3 (Al₂O₃/Na₂O = 1.0) and mix 4 (Al₂O₃/Na₂O = 1.5) showed numerous peaks that in mix 1 (control) and mix 2 (Al₂O₃/Na₂O = 0.5) were not present. This further supports the theory that the peaks representing minerals in the mix constituents did not participate in alkali-silicate reaction [11]. Another observation was noted at the edge of the curve, from 5° to 12° 2θ. This slight curve at the edge could result in the formation of meso-material of poorly crystalline nature with a pore size range of 20 to 50nm [5].

Furthermore, from the XRD analysis, no presence of geopolymer (N-A-S-H) phases were noted, since these are associated with broad peaks around 28° to 35° 2θ, and neither C-A-S-H phases, which are associated with main peaks at 30° 2θ [18]. The fly ash type F composition showed amorphous and crystalline substances such as mullite, which is a rare silicate mineral; hydrosodalite, a sodium aluminium silicate mineral, which is found in alkali rich igneous rocks; and a large amount of gibbsite.

Biomass bottom ash has already pozzolanic and self-cementing properties, and when mixed with water, hardens with an increase in strength properties with time. A slight hump was noted in mix 1 (control), centred approximately at 27° to 32° 2θ (Fig. 4). This diffused halo peak, defines the geopolymer systems [16]. This halo lost its curvature with mix 2 (Al₂O₃/Na₂O = 0.5), mix 3 (Al₂O₃/Na₂O = 1.0) and mix 4 (Al₂O₃/Na₂O = 1.5),
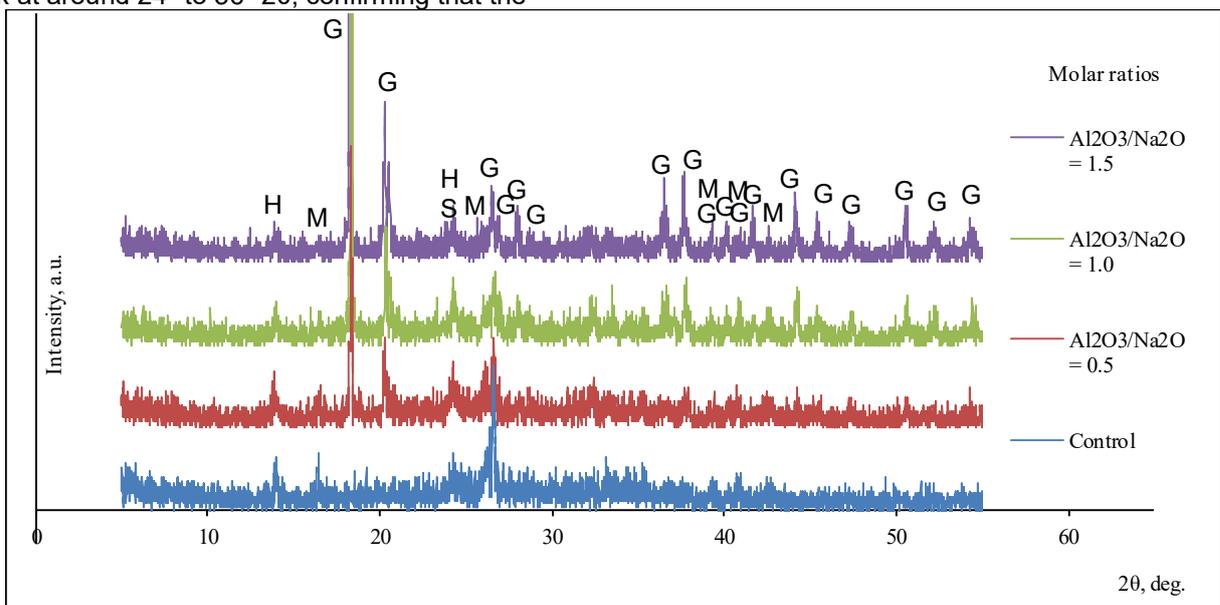

Fig. 3 - X-ray diffraction pattern of hardened geopolymer samples with type F fly ash. Notes: G – gibbsite (Al(OH)₃), M – mullite (Al(Al₁,₃·Si₀,₇·O₄,₉)(O₄)), HS - hydrosodalite (Na₄(Si₃Al₃O₁₂)(O₄)).
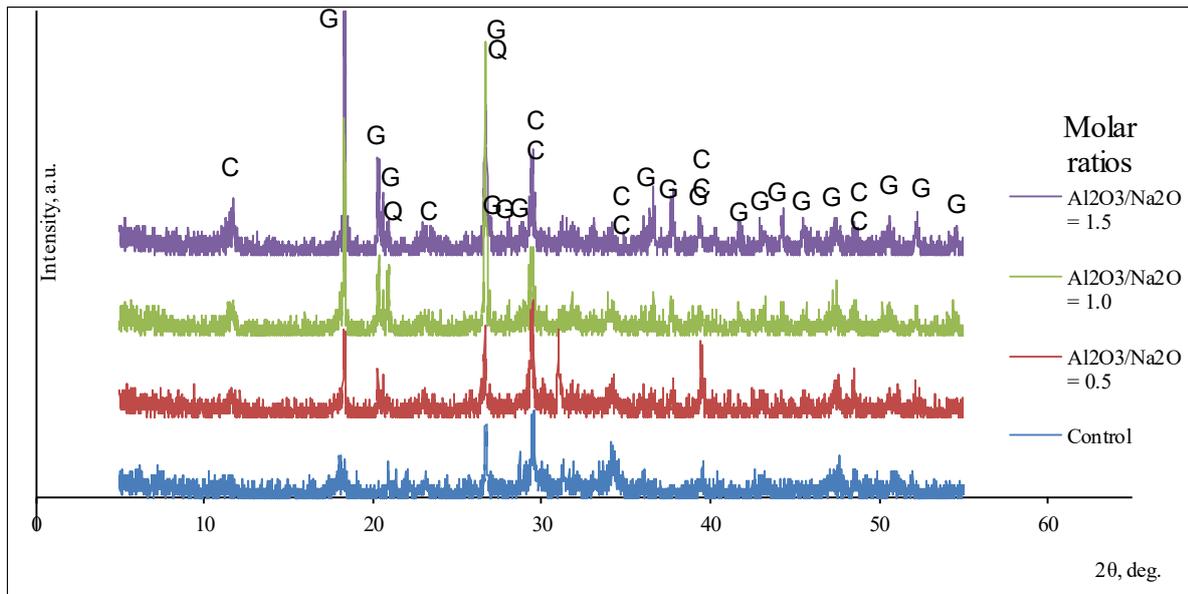
Fig. 4 - X-ray diffraction pattern of hardened geopolymer samples with biomass bottom ash. Notes: CA – calcium aluminium carbonate hydrate $Ca_4Al_2CO_9\cdot H_2O$, G – gibbsite $(Al(OH)_3)$, CC – calcite $(CaCO_3)$, Q – quartz (SiO_2).
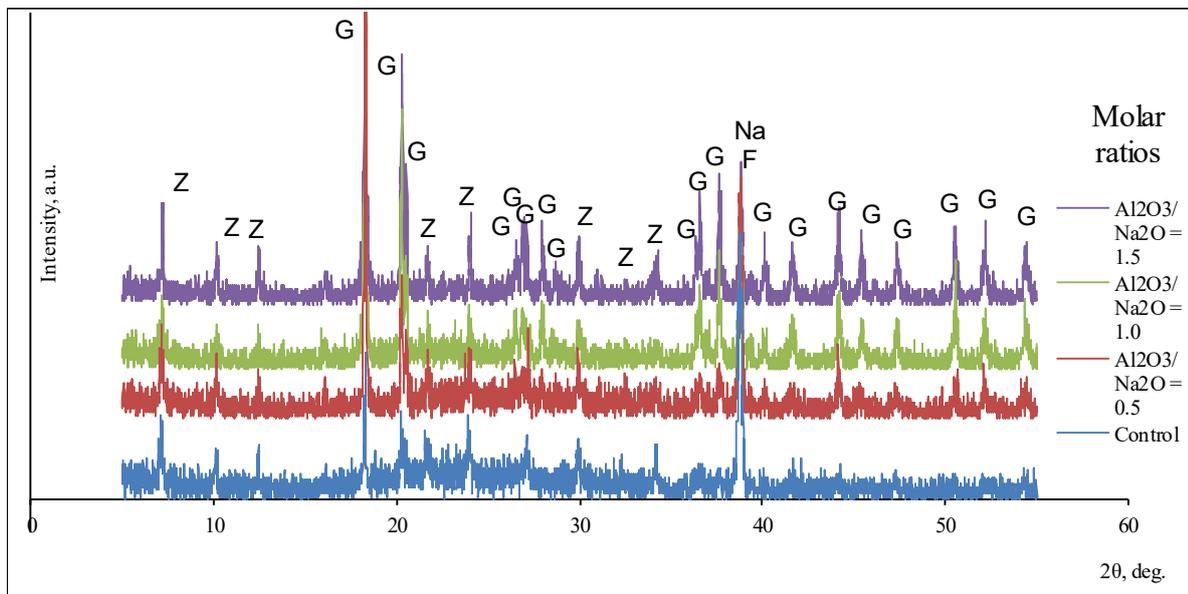

Fig. 5 - X-ray diffraction pattern of hardened geopolymer samples with ALF_3 production waste. Notes: Z – Zeolite A (Na) $(Na_2Al_2Si_{1.85}O_{7.7}\cdot H_2O)$, NaF – viliaumite (NaF), G – gibbsite $(Al(OH)_3)$.

confirming the loss of the geopolymerisation reaction. On the other hand, several peaks emerged with the addition of the $Al(OH)_3$ with some intense peaks at 18°, 27° and 29° 2θ (Fig. 4). The greatest intensity was observed at 18°, defined as the highest $Al(OH)_3$ molarity level [19]. These peaks showed crystal minerals within the sample that did not participate in the geopolymerisation system [11]. The common broad peak, defined in the region of 29° 2θ (Fig. 4), reveals the presence of aluminium substitution (C-A-S-H) phases, which was formed with additional activator containing calcium minerals. This addition can cause two separate reactions, a reaction forming geopolymer gel and a reaction forming calcium silicate hydrate (C-A-S-H) [10].

The XRD patterns were very similar in all three

figures with several peaks emerging with the addition of $Al(OH)_3$ while others diminished. A particular peak was observed at 12° 2θ, where in mix 1 this peak was very small; however with an additional quantity of $Al(OH)_3$ this peak increased in intensity in the molarity level of the calcium aluminium carbonate hydrate.calcite, peaking at 34° 2θ, showed a reduction in intensity with the addition of $Al(OH)_3$ (Fig. 4). At 27° 2θ, mix 1 (control) showed a small peak defined as quartz, whereby with time the intensity of the peak increased and became further enhanced with the addition of $Al(OH)_3$. Similar to fly ash, bottom ash also showed a curve at the edge of the graph, from 5° to 12° 2θ, showing the probability of the formation of meso-material of a poor crystalline nature with a pore size range of 20 to 50nm [5].

When comparing to the compressive strength results obtained for these mixes, it showed a decline in strength with the addition of the Al(OH)$_3$ whereby it was clear that geopolymerisation did not form with the addition of Al(OH)$_3$. XRD analysis further confirms this theory, since no amorphous phase was noted, but instead several crystalline peaks emerged in the analyses defining minerals that did not contribute to the geopolymerisation formation [5].

The biomass bottom ash composition showed amorphous and crystalline substances, such as quartz (silicon dioxide); calcium aluminium carbonate hydrate; calcite; and gibbsite, aluminium hydroxide.

The XRD analyses (Fig. 5) of hardened geopolymer samples with AlF$_3$ production waste showed a broad featureless hump centred approximately at 20° to 30° 2θ. The diffused halo peak, is caused by the amorphous aluminosilicate gel in the geopolymer system [16]. This halo peak had a shift from mix 1 (control) to mix 2 (Al$_2$O$_3$/Na$_2$O = 0.5), moving from 25° to 35° 2θ . This behaviour defines a disordered silica glass phase in the geopolymer system [5]. Several peaks, determining the crystalline minerals in the sample, were already present in mix 1 (control), but with the addition of Al(OH)$_3$ more peaks emerged in the analyses results. Common peaks were observed in all mixes defining NaF mineral at 38° 2θ, and declining in intensity when additional Al(OH)$_3$ was added to the mix. Another common peak for mix 2 (Al$_2$O$_3$/Na$_2$O = 0.5), mix 3 (Al$_2$O$_3$/Na$_2$O = 1.0) and 4 (Al$_2$O$_3$/Na$_2$O = 1.5) was observed at 18° 2θ and 20° 2θ, increasing in intensity with the addition of higher quantities of Al(OH)$_3$. The 18° 2θ peak showed the greatest intensity for higher Al(OH)$_3$ molarity levels [19].

In mix 3 (Al$_2$O$_3$/Na$_2$O = 1.0) and mix 4 (Al$_2$O$_3$/Na$_2$O = 1.5), the halo peak disappeared. This shows that the addition of Al(OH)$_3$ to the mixes prevented the geopolymerisation system from forming. Furthermore, comparing the compressive strength results obtained it was evident that there was a decline in compressive strength with the addition of Al(OH)$_3$, with the possibility of a crystalline zeolite formation instead of a geopolymer gel. In fact, zeolite was present in the control mix as shown in the XRD analyses. Moreover, mix 2 (Al$_2$O$_3$/Na$_2$O = 0.5), mix 3 (Al$_2$O$_3$/Na$_2$O = 1.0) and mix 4 (Al$_2$O$_3$/Na$_2$O = 1.5) showed numerous peaks that in mix 1 (control) were not present. This further promotes the possibility that the peaks representing minerals in the sample did not participate in the alkali-silicate reaction [11].

The AlF$_3$ production waste composition showed amorphous and crystalline substances, such as zeolite; sodium fluoride; and gibbsite.

Figure 6 shows the results obtained in terms of total porosity (%) and intruded volume (cc), with age. The total porosity percentage recorded for the fly ash Type F mixes, showed a similarity in

percentage whereby with time the porosity (%) experienced a reduction except for mix 2 (Al$_2$O$_3$/Na$_2$O = 0.5), which showed an increase in porosity percentage at 28 days. The common porosity values ranged between 31% and 80%, with some exceptions. The unusual % of mix 1 (control), 7 days' sample and mix 2 (Al$_2$O$_3$/Na$_2$O = 0.5), 28-day sample would need further investigation, since the difference recorded was very large compared to the other sample results.
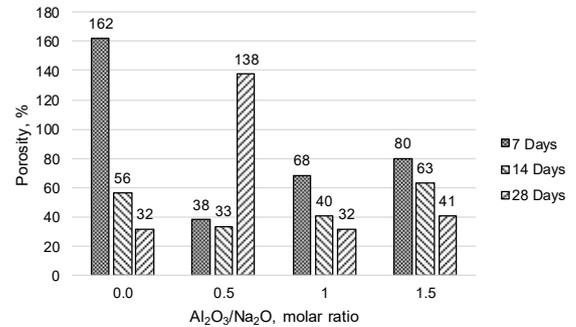

Fig. 6 - Porosity of hardened geopolymer samples with fly ash.

A trend in the total porosity (%) results was noted, whereby porosity decreased with time. Moreover, comparing these values to the compressive strength values of the geopolymer paste samples, showed that with decrease in porosity %, an increase in strength was observed.

Comparing the porosity (%) to the other two materials, fly ash was very close to biomass bottom ash porosity (%) (Fig.7).
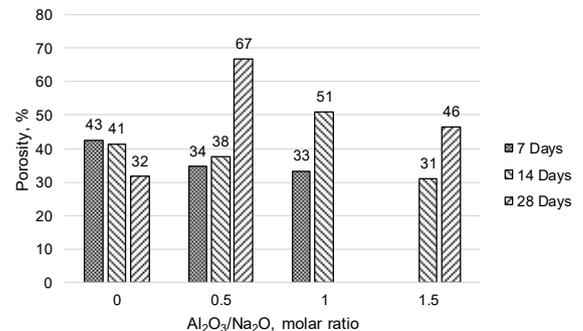

Fig. 7 - Porosity of hardened geopolymer samples with biomass bottom ash.

The total porosity percentage recorded for the biomass bottom ash mixes, showed a more consistent result than the fly ash, whereby with time the porosity (%) had an increase, except for mix 1 (control), which showed a decrease in porosity percentage at 28 days (fig. 7). The common porosity values ranged between 33% and 50%. These values were very consistent when compared to the fly ash.

The total porosity % results showed a possible trend, whereby Mix 1 porosity (%) decreased with time, while mix 2 (Al$_2$O$_3$/Na$_2$O = 0.5), mix 3 (Al$_2$O$_3$/Na$_2$O = 1.0) and mix 4 (Al$_2$O$_3$/Na$_2$O = 1.5) showed an increase in

porosity (%) with time. This is due to the addition of $Al(OH)_3$, whereby it contributed in increasing porosity within the sample structure.

Comparing these values to the compressive strength values of the geopolymer paste samples, showed that with decrease in porosity (%), an increase in strength was observed for mix 1 (control).

The total porosity (%) obtained from the analyses for AlF_3 production waste showed that this type of material, had a more porous structure than the fly ashes and biomass bottom ashes. Mix 1 and mix 3 showed a decrease in porosity (%) with time, while mix 2 (Al_2O_3/Na_2O = 0.5) showed an increase (fig. 8). mix 4 (Al_2O_3/Na_2O = 1.5) indicated a different behaviour, where porosity (%) decreased at 14 days and increased over the 7 days' sample at 28 days. The common porosity values ranged between 125% and 165%, with some exceptions showing higher and lower values in porosity (%).
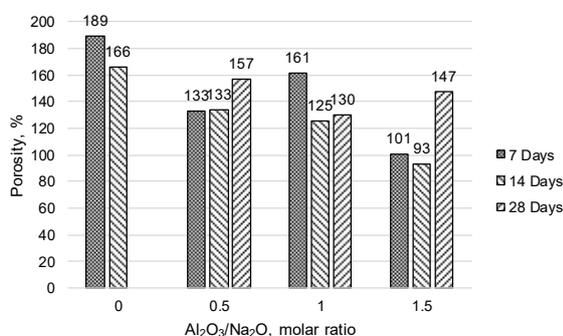

Fig. 8 - Porosity of hardened geopolymer samples with ALF_3 production waste.

The AlF_3 production waste (SiO_2) material mixes showed the highest total porosity (%) results when compared to the fly ashes and biomass bottom ashes mixes. Mix 1 (control) and mix 3 (Al_2O_3/Na_2O = 1.0) results obtained showed a similar trend, with porosity (%) decreasing by time. For mix 2 (Al_2O_3/Na_2O = 0.5) and mix 4 (Al_2O_3/Na_2O = 1.5), the trend changed and an increase in porosity (%) was noted by time. Comparing the porosity (%) results with the compressive strength results of the geopolymer paste samples, the decrease in porosity (%) showed an increase in strength, while an increase in porosity (%), showed a decrease in compressive strength. The reduction in porosity at 14 days and then the increase in porosity at 28 days can be compared to the increase in compressive strength at 14 days and reduction in strength at 28 days as explained above.

The average absolute density results of the samples showed an increase in value by time, but this increase does not reflect the porosity (%) results obtained.

6. Conclusions

The results obtained for the geopolymer paste samples based on the SiO_2/Na_2O ratio of 2.0,

showed an adequate performance for the control mix without additional $Al(OH)_3$, while the addition of the variant mixes, based on 0.5, 1.0 and 1.5 Al_2O_3/Na_2O ratios, showed a substantial decrease in strength for FA and BMBA. This is clearly observed for samples with BMBA ash and FA material. A comparable performance with the control mix was achieved for the PW waste material and samples with PW production waste haven't developed much strength.

It was shown in previous research that the addition of Al^{+3} ions, increased mechanical strength in geopolymers. In this research, the addition of $Al(OH)_3$ resulted in a reduction of the compressive strength. Therefore, further studies should be performed to investigate the performance of the $Al(OH)_3$ in the geopolymerisation process. All the samples were cured at 50°C for the entire 28 days.

The FA materials showed an increase in compressive strength with time.

FA showed a good performance during this study but the material failed in a brittle manner in compression. Further analysis on the elastic modulus of the mix is recommended.

The BMBA showed an increase in compressive strength with the reduction in activator, but further analyses would be required to assess the workability of the mix, since the mix of this material was slightly dry and without workability.

The PW (SiO_2) waste, showed a reduction in compressive strength at 28 days when compared with the 14 day results. Further investigations into the curing conditions including the curing environment and curing period for the PW (SiO_2) waste material are required.

FA samples showed tendency to decrease porosity with time with exception with mix 2 after 28 days, these high percentages, could be caused by defects in the samples analysed and/or internal cracking.

The bottom ash samples showed an increase in porosity while the AlF_3 production waste samples showed a high porosity when compared to the other waste materials; the samples for FA and BMBA were less porous then AlF_3 production waste.

REFERENCES

1. A. Islam, U. J. Alengaram, M. Z. Jumaat, I. I. Bashar, and S. M. A. Kabir, Engineering properties and carbon footprint of ground granulated blast-furnace slag-palm oil fuel ash-based structural geopolymer concrete - Constr. Build. Mater.,2015, **101**, 503.
2. D. Tavor, A. Wolfson, A. Shamaev, and A. Shvarzman, Recycling of industrial wastewater by its immobilization in geopolymer cement - Industrial and Engineering Chemistry Research, 2007, **46**(21), 6801.
3. M. Hu, X. Zhu, and F. Long, Alkali-activated fly ash-based geopolymers with zeolite or bentonite as additives - Cem. Concr. Compos., 2009, **31**(10), 762,
4. A. Heath, K. Paine, and M. McManus, Minimising the global warming potential of clay based geopolymers - J. Clean. Prod., 2014, **78**, 75.

5. U. Rattanasak and P. Chindaprasirt, Influence of NaOH solution on the synthesis of fly ash geopolymer - *Miner. Eng.*, 2009, **22**,(12) 1073.
6. M. O. Yusuf, M. A. Megat Johari, Z. A. Ahmad, and M. Maslehuddin, Effects of H_2O/Na_2O molar ratio on the strength of alkaline activated ground blast furnace slag-ultrafine palm oil fuel ash based concrete - Mater. Des., 2014, **56**, 158.
7. J. S. J. Van Jaarsveld, J.G.S., Van Deventer, Effect of the Alkali Metal Activator on the Properties of Fly Ash Based Geopolymers - Ind. Eng. Chem. Res. *,* 1999, **38,** 3932.
8. M. Mikoč, I. Bjelobrk, and J. Korajac, Alkali activated fly ash concrete - Tech. Gaz., , 2011, **18**(1), 99.
9. Z. Pan *et al.*, Damping and microstructure of fly ash-based geopolymers - J. Mater. Sci., 2013, **48**(8), 3128..
10. P. Nath and P. K. Sarker, Effect of GGBFS on setting, workability and early strength properties of fly ash geopolymer concrete cured in ambient condition - Constr. Build. Mater., Sep. 2014, **66**, 163.
11. A. Grinys, V. Bocullo, A. Gumuliauskas, Research of Alkali Silica Reaction in Concrete With Active Mineral Additives - Sustaible Architecture ans Civil Engineering, 2014 **,1**(6).
12. S. Riahi, A. Nazari, D. Zaarei, G. Khalaj, H. Bohlooli, and M. M. Kaykha, Compressive strength of ash-based geopolymers at early ages designed by Taguchi method - Mater. Des. , 2012, **37**, 443.
13. J. June *et al.*, Geopolymer Concrete with Fly Ash, Second Int. Conf. Sustain. Constr. Mater. Technol., 2010, **7**(6), 1493.
14. M. Olivia and H. Nikraz, Properties of fly ash geopolymer concrete designed by Taguchi method - *Mater. Des.* , 2012, **36**, 191.
15. D. Vaičiukyniene, V. Vaitkevičius, A. Kantautas, and V. Sasnauskas, Effect of AlF3 production waste on the properties of hardened cement paste - Material science, 2012, **18**(2), 187.
16. J. L. Provis, G. C. Lukey, and J. S. J. Van Deventer, Do geopolymers actually contain nanocrystalline zeolites? a reexamination of existing results - Chem. Mater. , 2005, **17**(12), 3075.
17. N. Saidi, B. samet, S. Baklouti, Effect of Composition on structure and mechanical properties of metakaolin based PSS-geopolymer - International Journal of Material Science, 2013, **3**(4), 145.
18. S. Pangdaeng, T. Phoo-ngernkham, V. Sata, and P. Chindaprasirt, Influence of curing conditions on properties of high calcium fly ash geopolymer containing Portland cement as additive - Mater. Des., 2014, 53, 269.
19. G. S. Ryu, Y. B. Lee, K. T. Koh, and Y. S. Chung, The mechanical properties of fly ash-based geopolymer concrete with alkaline activators - Constr. Build. Mater., 2013, **47**, 409.

****

MANIFESTĂRI ȘTIINȚIFICE / SCIENTIFIC EVENTS

10th ACI/RILEM INTERNATIONAL CONFERENCE ON CEMENTITIOUS MATERIALS AND ALTERNATIVE BINDERS FOR SUSTAINABLE CONCRETE

Former CANMET/ACI International Conference on Fly Ash, Silica Fume, Slag, Natural Pozzolans and Alternative Supplementary Cementitious Materials in Concrete

The purpose of this international conference is to present the latest available scientific and technical information in the field of supplementary cementitious materials and novel binders for use in concrete. The new aspect of this edition is to highlight advances in the field of alternative and sustainable binders and supplementary cementitious materials, for which the research is growing in importance.

Original papers on all aspects of pozzolans, mineral admixtures, standard and alternative supplementary cementitious materials are invited to be presented at the conference and be published in the proceedings.

Key topics:
- Microstructure and hydration
- Multi-component binder systems
- Alternative supplementary cementitious materials
- Alkali activated materials
- Alternative binders
- Nanomaterials
- Chemical admixtures
- Concrete mix designs for sustainable development
- Rheology
- Curing techniques
- Mechanical performances and durability
- Modeling of concrete properties
- Life-cycle analysis
- Service life
- Standard and test method development
- Case studies
- Special concrete
- Biosourced materials
- Recycled materials

****